CERN Summer Student Programme 2023

15 September 2023
ukuluhari@gmail.com

ATLAS Technical Coordination WAterLeakDetection project (WALD)

Uku Luhari - *CERN*

Supervisor:
Florian Haslbeck - *University of Oxford, CERN*

Keywords: A Toroidal LHC ApparatuS (ATLAS), Detector Safety System (DSS), Smart Paper, Technical Coordination, water leak detection,.

Abstract

The detection of water leaks inside the service caverns of ATLAS detector is a critical concern due to potential damage to sensitive electronics. Sensing wires are used to monitor the detector and its infrastructure. To improve the detection of small leaks that have increased recently due to the corrosion of pipe joints, the Technical Coordination Water leak project developed and deployed a novel water leak detector based on "Smart Paper" developed by the University of Washington. The new material combines cellulose and carbon nanotubes yielding a paper-like whose intrinsic resistance increase by the order of several thousand percent upon absorption of liquids. The material's texture enables the installation of the detector in complicated geometries like for example being wrapped around joints. This summer student project investigated the intrinsic resistance during absorption and drying of the material to provide data to model the response. The model can be used for detector optimisation, degradation studies and to enhance the so-far binary leak detection with an estimation of the amount of detected water.

Contents

1 Introduction

ATLAS [1] is one of the four large experiments at the LHC [2]. The detector is situated circa 100 m underground inside an experimental cavern, its support infrastructure is situated both on the surface as well as in two underground service caverns. The possibility of water leaks arising in the cooling system present a significant risk to the delicate electronics and equipment. ATLAS observed 191 water leaks from 2017 to 2022, where only few actually damaged equipment. Therefore, the Detector Safety System (DSS) [3, 4] employs sensing wires to detector leaks and take counter measures [5].
To improve the monitoring capacities of the wires that are routed on the ground and the false floors to faster detect small leaks that have arisen recently at corroded joints, the ATLAS Technical Coordination Water leak detection project developed a new water leak detector [6] in collaboration with the University of Washington [7] using "Smart Paper" [8] , a novel water-sensitive cellulose based material. Upon absorption of liquids, the cellulose fibers within the paper expand which increases the intrinsic resistance of the material by a factor of several thousand with respect to the dry state. The materials flexibility enable a placement within intricate 1D and 2D geometries, for example, samples can be wrapped around pipe fittings, applied within racks, or fixed to heat exchangers.

The scope of this summer student project was to develop a model of the material's response to liquids to better understand the optimal detector geometry and to understand the material in extreme conditions. Furthermore, the project investigated if the amount of water detected by a sample can be deduced from the detector's response.

2 Measurement setup

A measurement setup, see Figure 1, was developed that simultaneously record the resistance, the relative wet area of the sample and the weight of the sample and the water. The shape and area of the water was previously found to have a significant influence on the response of the material [9].

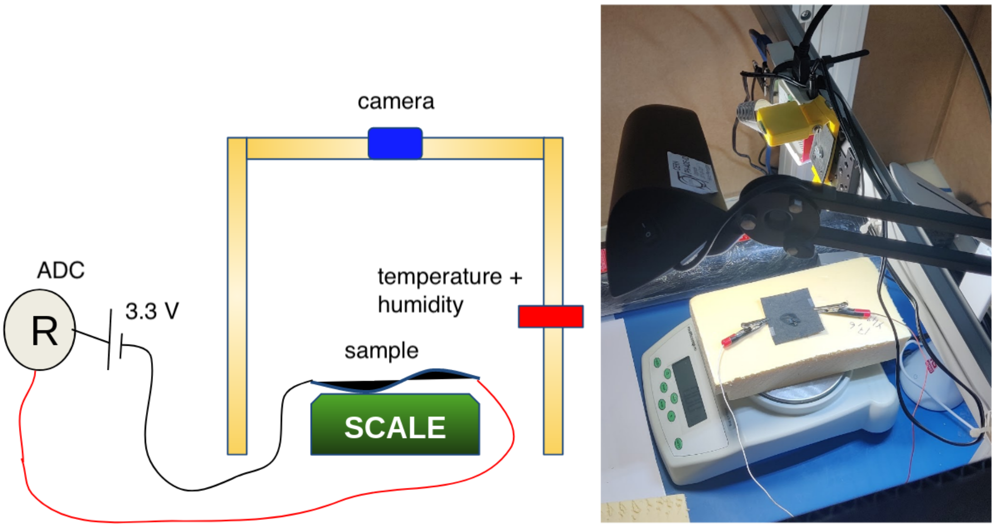

Figure 1: Sketch (left) and photo (right) of the measurement setup with a small sample with water. The camera is mounted inside the yellow frame.

The sample's resistivity is measured by applying 3.3 V with crocodile clips. For the readout the WALD readout module is used featuring a commercial differential ADC (ADS1115-Q1, 16-bit [10]) in single ended mode [11]. The sample is placed on a digital scale to measure the amount of water on the sample with a resolution of 0.01 g (Multicomp PRO 800 x 0.01 g [12]). The cable weight is subtracted by taring. The wet area is estimated from photos taken by Raspberry Pi Camera Module 2 [13]. The camera is mounted on top of the sample in a 3D printed frame and readout by a Raspberry Pi 4. Two lamps (CFL [14] and LED [15]) provide illuminate the sample from different angles and reduce shadows to ease the determination of the wet area. The setup is shielded from the environment (e.g. air conditioning) by placing a large carton box on top it. A temperature-humidity sensor (Adafruit AM2315 [16]) logs the environmental conditions.

2.1 ADC calibration

The five lowest gains (2/3, 1, 2, 4, 8) of the ADC are calibrated to Ohm as the response is non-linear with respect to the input resistance, as the resistance is measured in parallel with the input stage. The gain must be chosen accordingly to the sample size as smaller samples have a smaller intrinsic resistivity. Different reference resistance values in approximate steps of 10 $k\Omega$ up from 0 - 150 $k\Omega$ are used. The response is fitted with different degree polynomial functions:

$$\text{resistance}(\text{adc}) = \text{polynomial}(\text{adc}) \tag{1}$$

The calibration constants are chosen based on a combination of the χ^2_{red} value ($\chi^2_{red} = \chi^2/\text{NDF}$) and the lowest possible polynomial [11]. An example for Gain 1 is shown in Figure 2.

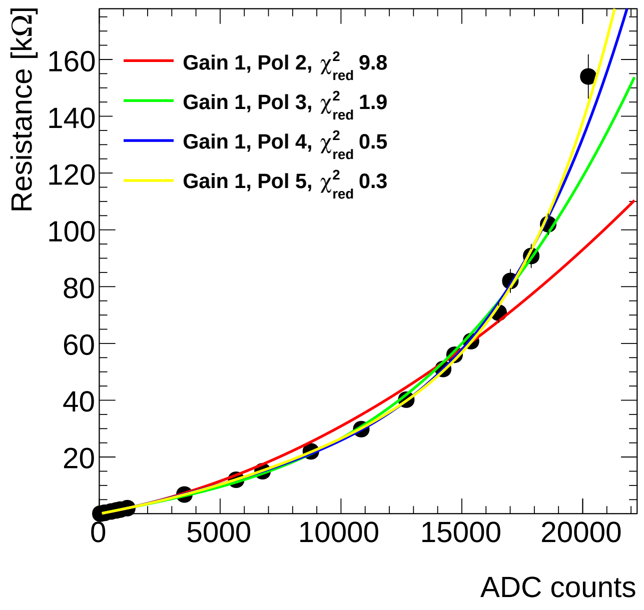

Figure 2: Resistance vs ADC counts for Gain 1 with different degree polynomials fit to the data.

Table 1 lists the best gain recommendation given a certain sample size. The gain is chosen to provide the best sensitivity in the resistance for 5 drops of water. Gain 4 is preferred for smaller samples (70 × 100 mm^2, 35 × 116 mm^2) and Gain 2 is preferred for larger samples (50 × 300 mm^2).

Outer dimensions			Gain	Resistance [kΩ]		
W [mm]	L [mm]	Area [mm^2]		dry	1 drop	5 drops
70	100	7000	4	1.23	1.18	2.44
35	116	4060	4	1.55	2.02	8.81
50	300	15000	2	5.89	6.84	15.76

Table 1: Gain recommendation for different sample sizes. 1 drop corresponds to 0.05 ml.

2.2 Readout

The readout script calls every 30 s containerised scripts to record the resistance, the weight, the temperature, the humidity and the calculated wet area. The area estimation algorithm was developed during the project:

- The image is cropped manually at the beginning of a measurement to have a unicolor background.
- Using the canny edge algorithm provided by the open-cv python framework [17] the sample outline is found. The canny algorithm spots edges by blurring the image,

calculating gradients, suppressing non-maximum gradients, applying double thresholds and then tracks continuous edges to find shapes.

- The largest found rectangle is taken as the sample outline and used as a mask.
- The image is converted to black and white with adjustable thresholds. Since the wet patch on the paper is darker than the surrounding sample, counting the white and black pixels inside the mask returns the percentage of wet area on the sample.

2.3 Measurements

Between 20.07.2023 - 25.08.2023, around 70 measurement runs were taken for different sample sizes (55x55 mm, 116x35 mm, 95x90 mm, 250x50 mm, 250x20 mm, 250x100 mm) and different amounts of water (1, 3, 5, 10 and 15 drops). On average, one measurement took about 1.5 hours. The data is stored in csv format. The pictures in png.

3 Results

3.1 Soaking-drying process

Figure 3 shows as an example the response in terms of the resistance in Ohm of a 250×100 mm sample to five drops of tap water, per relative wet area for both absorbing and drying. Clearly, the response during soaking and drying is significantly different. The time axis is included by marking every 2.5 min with a red marker.

1. The sample is dry.
2. Once the water is placed on the sample, the resistance increases with relative wet area.
3. During the initial absorption the wet area only slowly increases as the water is absorbed faster in the vertical direction, while the resistance increases fast (additionally marked in orange). This is not observable the case for small amounts of water (1 drop) with a measurement interval of 30 s.
4. Once the paper is saturated throughout the thickness, the absorption continues horizontally to the surface of the paper and the resistance further increases/
5. Once the maximum wet area is reached, the resistance peaks. Sometimes, the maximum resistance shortly after the maximum area is reached (between points 5 and 6).
6. The material starts drying from the surface, thus the resistance decreases slowly than the wet area decreases relatively faster as it was the case for the absorption process.

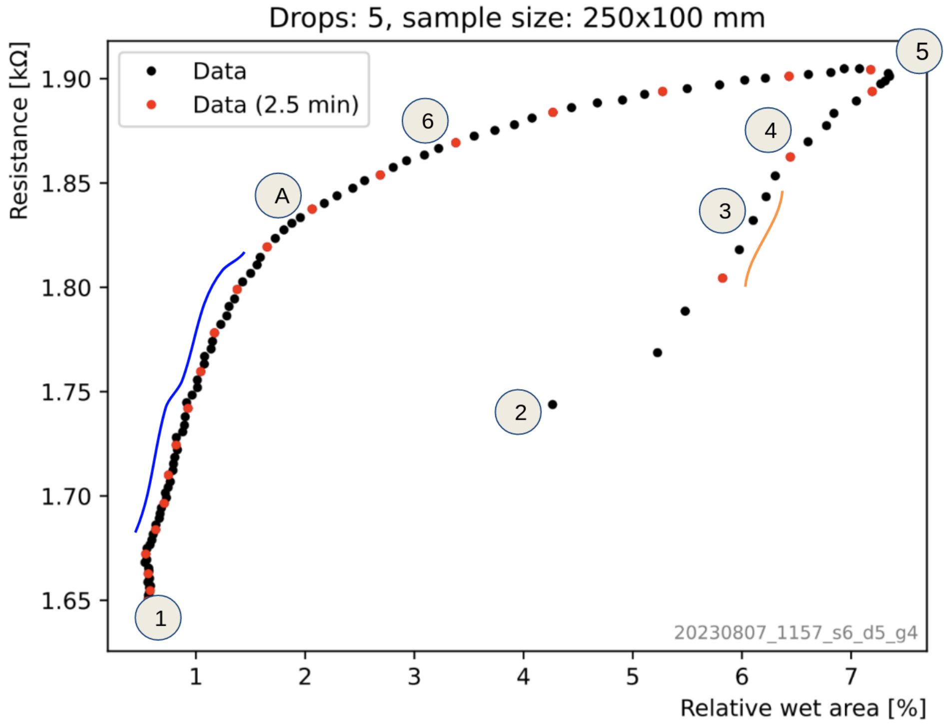

Figure 3: Soaking and drying response in Ohm per relative wet area for a sample. The time can be read from the red markers that indicate every 2.5 min.

7. Once the "core" starts drying, the resistance decreases much faster while the relative wet area only decreases very slowly.

While the overall behaviour is similar for all measurements, it is observed that the shape of the soaking-drying curve changes with the amount of water on the sample, see Figure 4. For large amount of water, the maximum relative wet area is reached even before the maximum resistance if the sample is completely covered in water. Adding more water to the sample seems to ...

- ... amplify the absorption plateau. There is more water sitting on top of the paper waiting to be absorbed and it stretches the graph wider in the process.
- .. lower the point A (in Figure 3). The resistance peaks more for a larger relative wet area.
- .. cause the vertical part of drying curve (blue line in Figure 3) to be more slanted. This part gets more vertical the less water there is on the sample - 4.

Additionally, the whole curve is usually more streamlined if the sample is not long and narrow but rather has connected sides of similar length - water accumulation in the same spot is less prevalent (but it depends noticeably on the creases in the paper). Also, longer and narrower samples are more sensitive since the change in resistance is much more noticeable when the water manages to cover the whole width of the sample.

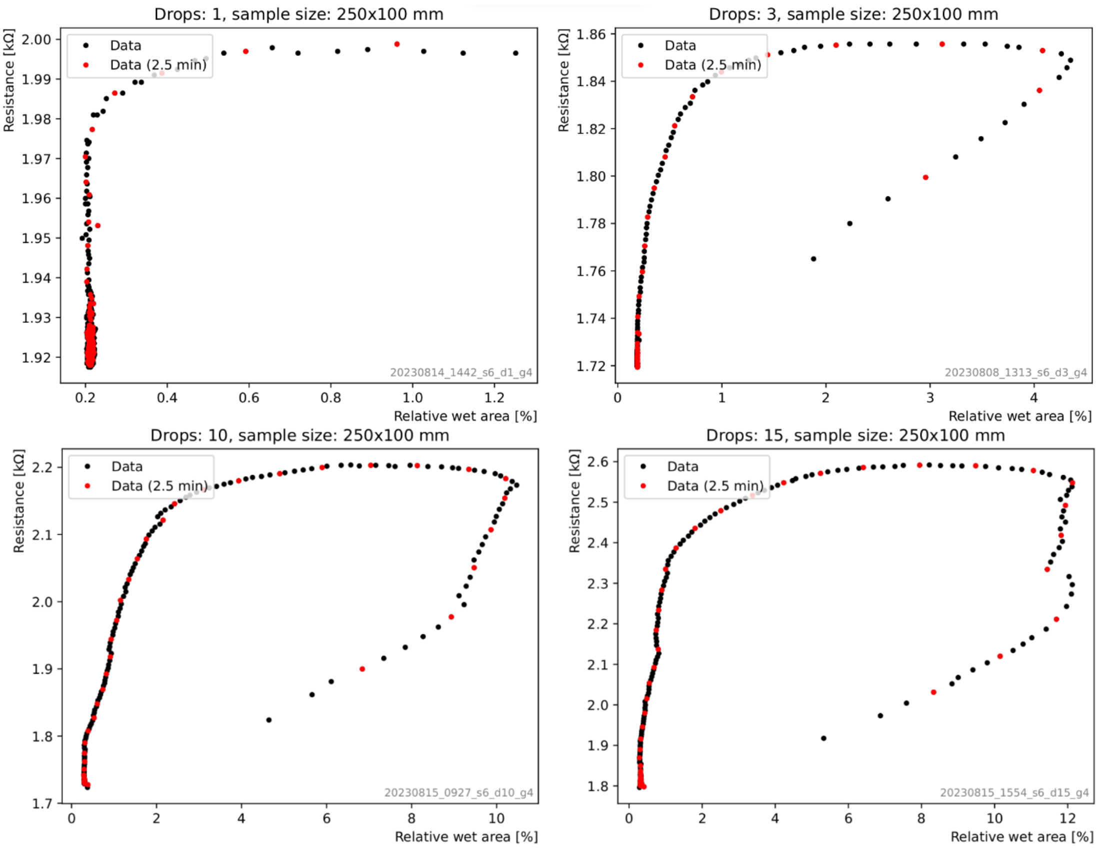

Figure 4: 250x100 mm sample with different amount of drops

3.2 Estimation of the amount of water

Figure 5 presents the maximum wet area, the time until the maximum resistance is reached and the maximum relative resistance change as a function of the number of drops (1 drop $\approx 0.05\,\mathrm{g}$) for different samples. All three observables show a positive correlation with the number of drops. For deployed sensors, only the resistance over time is available to determine whether a leak has occurred or not. The plot showing the time until the maximum resistance and the maximum relative resistance for a $250 \times 100\,\mathrm{mm}$ sample show that it appears to be possible to not only model the response approximately but also infer the amount of water.

Figure 6 shows for different sample sizes the time until maximum resistance versus the absolute change in resistance. The plots reveals a discernible pattern suggesting a substantive correlation between the quantity of water present on the sample and both the change in resistance and the time it took to attain peak resistance. The groups of data points representing different amounts of water are fairly isolated from each other and it becomes therefore possible to assume the size of the leak, only by the resistance readout from the leak detection system. Furthermore, it is evident that thinner samples show a larger response to than wider as the full width can be soaked for smaller amounts of water.

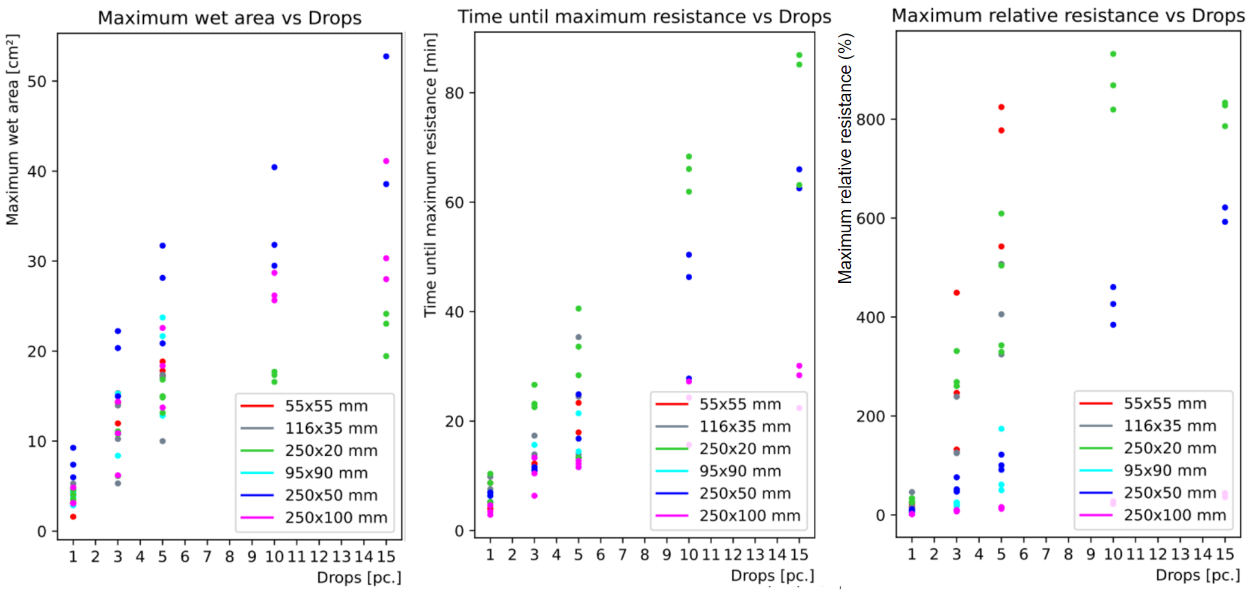

Figure 5: Maximum values for 250x100 mm sample

3.3 Improvements

The relative wet area estimation has currently an uncertainty of about 20 % of the estimated value. Furthermore, the crocodile clamps are not always on the same place, water is not dropped onto the paper exactly at the same time or at the exact same location and so on. The water was always dropped in the vicinity of the center of the sample, but the inconsistency can be caused by manual application.

4 Conclusion and outlook

This summer student project investigated the relation between water content and intrinsic resistance during absorption and drying of "Smart Paper" within the scope of the Technical Coordination water leak project. Several measurements were carried out, adding the measurement of the weight and the relative wet area of a sample as visible from the surface. The measurements yield results compatible with expectations, and can be used to model the soaking and drying of a sample given the amount of water applied to it. The next step will be to observe and extract an inverse relationship between the resistance and the size of the patch, based on the size of the sample and the amount of water applied to it to improve the water detection algorithm.

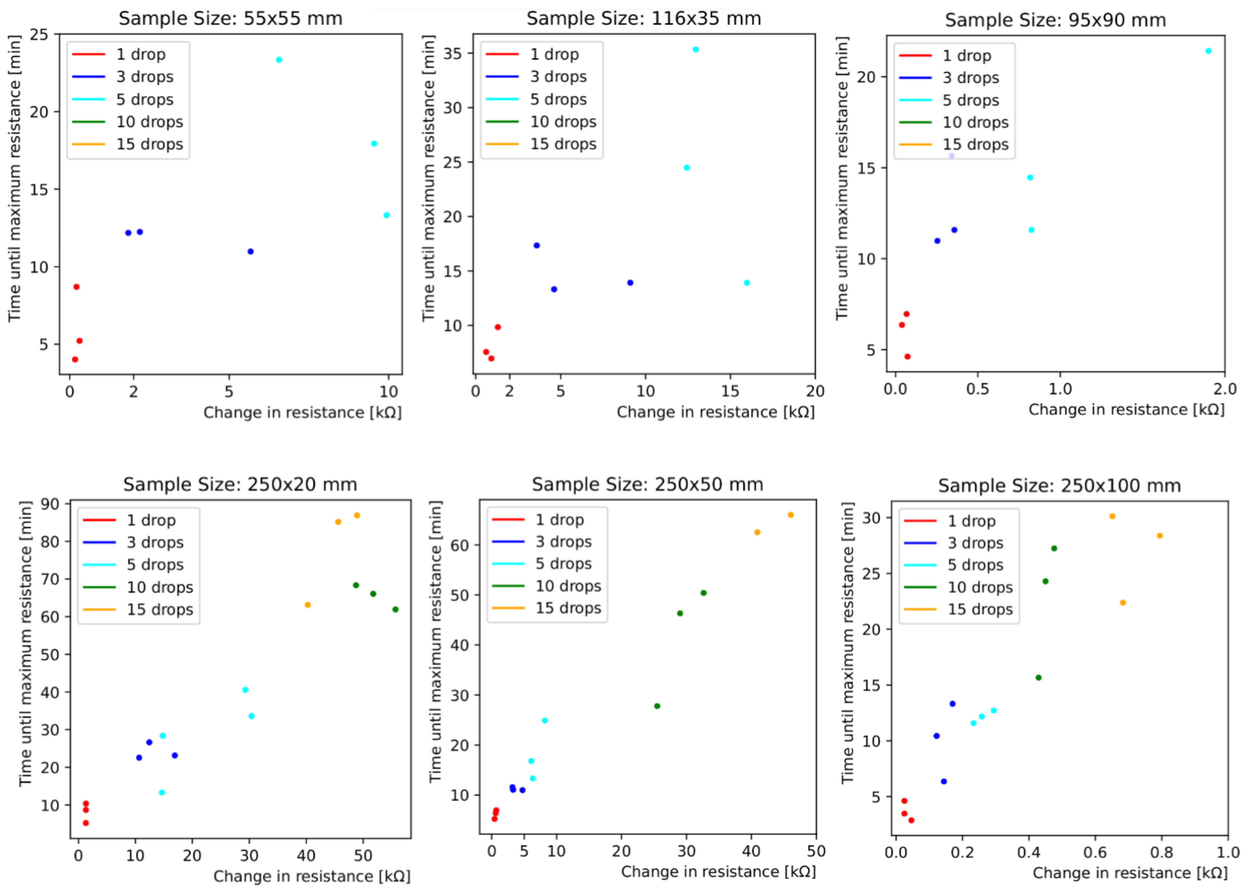

Figure 6: Change in resistance VS Time until maximum resistance for 6 different sample sizes

References

[1] ATLAS Collaboration. 'The ATLAS Experiment at the CERN Large Hadron Collider'. In: *Journal of Instrumentation* 3.08 (2008), S08003. DOI: 10.1088/1748-0221/3/08/S08003.

[2] Lyndon Evans and Philip Bryant. 'LHC Machine'. In: *Journal of Instrumentation* 3.08 (Aug. 2008), S08001. DOI: 10.1088/1748-0221/3/08/S08001.

[3] Stefan Luders et al. 'The CERN Detector Safety System for LHC Experiments'. In: *Proceedings of ICALEPCS2003, Gyeongju, Korea*. TH214. URL: cds.cern.ch/record/1054106.

[4] O. Beltramello et al. 'The Detector Safety System of the ATLAS experiment'. In: *Journal of Instrumentation 4.09* (Sept. 2009). DOI: 10.1088/1748-0221/4/09/p09012.

[5] C. Solans. *Water leak detection implementation in USA15*. 2019. URL: edms.cern.ch/document/1814569/.

[6] C. Solans. *RELIANCE Water Leak Detection System in ATLAS*. 2021. URL: edms.cern.ch/document/2423056.

[7] Sheila M. Goodman et al. 'Scalable manufacturing of fibrous nanocomposites for multifunctional liquid sensing'. In: *Nano Today* 40 (2021), p. 101270. ISSN: 1748-0132. DOI: doi.org/10.1016/j.nantod.2021.101270.

[8] A. B. Dichiara et al. 'Smart papers comprising carbon nanotubes and cellulose microfibers for multifunctional sensing applications'. In: *J. Mater. Chem. A* 5 (38 2017), pp. 20161–20169. DOI: 10.1039/C7TA04329E.

[9] Ignacio Asensi Tortajada. 'Design and Development of Safety and Control Systems in ATLAS'. In: (2021). Presented 09 Nov 2021. URL: cds.cern.ch/record/2791748.

[10] Ti. *Automotive 16-bit, 860-SPS, 4-ch, delta-sigma ADC with PGA, oscillator, VREF, comparator and I2C*. www.ti.com/product/ADS1115-Q1. 2023.

[11] F. Haslbeck et al. *Reliance resistance measurement calibration*. 2023.

[12] *Digital Scale MP700628A*. ch.farnell.com/multicomp-pro/mp700628/compact-balance-800g-0-01g/dp/3583603. 2023.

[13] *Raspberry Pi Camera Module 2*. URL: www.raspberrypi.com/products/camera-module-v2/.

[14] *Luxo New Verit Task Light, Part Number 16424BK*.

[15] *RS PRO LED Desk Lamp, 1.8 W*. 2023. URL: uk.rs-online.com/web/p/desk-lamps/1363723.

[16] *Adafruit AM2315 Encased I2C Temperature/Humidity Sensor*. URL: www.adafruit.com/product/1293.

[17] Open CV. *Canny edge detection*. 2023. URL: docs.opencv.org/3.4/da/d22/tutorial_py_canny.html.